Interferential Current Stimulation for Non-Invasive Somatotopic Sensory Feedback for Upper-Limb Prosthesis: Simulation Results using a Computable Human Phantom

Leen Jabban, Dingguo Zhang and Benjamin W. Metcalfe*

***Abstract*— The addition of sensory feedback to upper-limb prostheses has been shown to improve several aspects of the user experience. In an attempt to create an intuitive sensory feedback method, transcutaneous electrical stimulation of the stump has been used to elicit referred sensation in the phantom hand by stimulating the underlying nerves. However, the sensation at the electrodes is always reported due to the stimulation of mechanoreceptors. This work investigates the use of interferential stimulation (the superposition of two kilohertz-frequency stimulation currents to form a low-frequency envelope stimulation waveform) to produce focused and selective stimulation that reduces the sensation at the electrodes. A computable human arm phantom model was used to analyse the electric fields created by interferential stimulation against those created by low-frequency stimulation. The results support the assumption that interferential stimulation could result in reduced sensation at the electrode. However, they did not show benefits in terms of penetration at the frequency range considered. In fact, the results suggest that slightly higher currents may be required.**

I. INTRODUCTION

Sensory feedback has been shown to be a beneficial addition to upper-limb prostheses as it improves the performance in challenging tasks, increases embodiment and reduces phantom limb pain [1]. A range of invasive and non-invasive methods have been suggested with invasive methods leading in terms of the ability to elicit more natural, referred sensations. Non-invasive methods, however, are an important area of research as implanted methods require considerable development before being available commercially and, even when they are, some users may wish to try sensory feedback before undergoing surgery, and others may not wish to undergo surgery at all.

Somatotopic feedback is thought to be more intuitive, reducing the cognitive effort required. One of the non-invasive methods proposed recently is electrical stimulation through surface electrodes placed at locations providing access to superficial nerves. Those locations can result in a less selective, but non-invasive stimulation of the peripheral nerve, and thus the production of referred sensations. However, in addition to the referred sensation, a sensation at the electrodes is always reported [2], [3]. This paper proposes the use of interferential stimulation (IFS) to reduce the sensation felt at the electrodes.

The principle of IFS (also referred to as temporal interference stimulation) is illustrated in Figure 1 (A). The setup includes two electrically isolated stimulation sources (f_1 and f_2), each supplying a sinusoidal kilohertz-frequency stimulation current. The superposition of the two fields creates an envelope waveform with a frequency matching the beat frequency ($\Delta f = f_1 - f2$). The rectification properties of the neural membranes limit the activation of the nerves to areas of maximal interference [4]. This ability to limit the stimulation location to an area remote to the electrodes improves the focality of the stimulation [5]. The location of near-perfect temporal interference can be controlled by changing the strength of the different stimulating fields enabling steerability of the stimulation area. Another advantage of using high-frequency stimulation is the reduced skin impedance at kilohertz frequency, improving penetration [6].

IFS has been used in physical therapy to reduce the effect of skin impedance. However, the resulting waveforms have not been studied [6]. Initial experiments were used to test the idea of using IFS for sensory feedback. The results supported the theory showing that the subjects did not feel the stimulation when the sources had the same frequency, but were able to follow the beat frequency when they were different [7]. Furthermore, it was shown that the phase difference between the two AC sources could be used to move the location of the perceived sensation along the arm [8]. The use of IFS for deep brain stimulation has gained interest recently. Grossman et al. carried out a series of experiments including computational modelling, physical experiments and in-vivo experiments in mice to confirm the steerability of the stimulation location [9]. Moreover, Li et al. have shown the suitability of IFS for selective neuromuscular activation in the arm through a cuboid computational model and tests on healthy subjects [10].

This paper uses a high resolution computational human phantom model to simulate IFS. The aim of the simulation is to demonstrate preliminary results comparing the electric field obtained within the arm when low frequency stimulation is used against IFS in terms of penetration, focality and steerability.

II. METHODS

A. Software and Computable Human Phantom

Sim4life (Zurich MedTech AG) was used to carry out the simulation. Sim4life is a computational modelling software designed for life science applications. The use of Sim4life enables access to high-resolution anatomical models [11] with preset biological material properties [12]. The model

Leen Jabban, Dingguo Zhang and Benjamin W. Metcalfe are with the Department of Electronic and Electrical Engineering, University of Bath, Ba2 7AY, Bath, United Kingdom BWM23@bath.ac.uk

Yoon-sun (cV3.1) was used to simulate the effect of electrodes placed on the upper-arm to stimulate the Ulnar and Median nerves. A $\sim$10 cm section of the upper-arm was used to create the finite element model.

B. Simulation Setup

An array of six electrodes was placed around the arm, as shown in Figure 1 (B). The placement of the electrodes was chosen to maximise access to the Median and Ulnar nerves (highlighted). The electrodes were set as Dirichlet boundary conditions with a fixed voltage. The material properties of the arm were pre-set, as mentioned earlier [12]. The voxels were created based on a uniform grid with a step size of 0.5mm. The grid size was not required to be finer at the electrode-skin interface as the electrodes were modelled as perfect conductors, simplifying the interface between the electrodes and skin. Finite element modelling was used to solve the quasi-electrostatic equation ($\nabla \cdot \sigma \nabla \phi = 0$) where σ is the local electrical conductivity, and ϕ is the electric potential. The strength of the electromagnetic field within the simulated body is then calculated using $\vec{E} = -\nabla\phi$. The field obtained was then scaled to enable the stimulation current to be set (see Appendix for current calculation).

The sum of the fields was obtained by adding the components of each field along the three axis and calculating the absolute magnitude of the resultant field. This sum was considered to be the sensation-inducing field for the low frequency stimulation (LFS). The maximum amplitude of the temporal interference ($\vec{E}_{Env}^{max}$) of the two scaled fields is obtained using equation (1), as described by Grossman et al. [9]. The interference field was considered to be the sensation-inducing field for the IFS.

$$\left|\vec{E}_{Env}^{max}\right| = \begin{cases} 2|\vec{E}_2| & if|\vec{E}_2| < |\vec{E}_1 cos(\alpha) \\ \frac{2|\vec{E}_2 \times (\vec{E}_1 - \vec{E}_2)|)}{|\vec{E}_1 - \vec{E}_2|} & otherwise \end{cases} \quad (1)$$

C. Assessment Criteria

In order to determine the benefit of IFS in comparison to LFS, three different assessments were carried out. To start with, the frequency was increased and the material conductivity at each frequency was adjusted. Without scaling the field, as current stimulation accounts for the change in resistance, the maximum electric field intensity at the Median and Ulnar nerves was measured. This was used as an assessment of the effect of increased frequency on the penetration of the field through the skin and other biological tissues.

The second test was designed to assess whether IFS results in reduced sensation at the electrodes. The increased electric field spread in the skin is assumed to activate mechanoreceptors and nerve endings, resulting in more sensation below the electrodes. Given that a uniform mesh is used, the sum of the magnitudes of the different sensation-inducing fields at different nodes was chosen as a measure of the distribution of the field between the different tissues.

The third test was designed to assess steerability and the strength of the IFS field at the nerves compared to LFS. The ratio of the two currents applied (I_a and I_b) was changed while keeping the sum constant ($= 5$mA). The maximum generated field at each of the nerves was then calculated. The results were used to compare the maximum achievable magnitudes and selectivity. A selectivity measure (S) was introduced, as shown in equation (2) and was calculated for different current ratios (I_r).

$$S(I_r) = 20\log_{10}\left[\frac{max(E_t(I_r))}{max(E_o(I_r))}\right] \quad (2)$$

Where E_t and E_o are the field intensity at the target and off-target nerves, respectively.

The tests were repeated with different electrode setups to assess the variability of the results. Setup A used pairs of electrodes (1,3) and (2,4) to deliver current I_a and I_b, respectively. Similarly, setup B used pairs of electrodes (1,3) and (4,6). The distance between the same circuit electrodes in both setups is similar, but the distance between the pair is greater in setup B than A where they are interlocked.

III. Results

A. The effect of higher frequency on penetration

Figure 1 (B) shows the effect of increased frequency on the maximum electric field intensity at the different nerves with a voltage of $\pm$10V applied at the electrodes. It can be seen that using frequencies in the range of $1-5$kHz does not result in an increased field intensity at the nerves. In fact, a 9% decrease in field intensity at the Median nerve is seen moving from 100Hz to 2kHz. The effect of higher frequency on increased penetration is seen at frequencies above 10kHz where the field intensity at the nerves starts increasing due to the increased overall conductivity between the electrodes and nerves. This matches the literature results where high-frequency stimulation ($<$ 10kHz) did not result in a decrease in the stimulation threshold [6].

B. The effect of IFS on the spread of the sensation-inducing electric field

Figures 1 (D) (ii) and (E) (ii) show the distribution of the sensation-inducing field within the different tissue types when IFS (top) and LFS (bottom) is used. The results were obtained using $I_a = I_b = 2.5$mA. It can be seen that IFS results in lower field distribution in the skin, both in terms of percentage and magnitude. The cross-sectional snapshots in Figures 1 (D) (iii) and (E) (iii) enable the visualisation of the fields. The reduced spread of the field in the skin is expected to result in reduced activation of mechanoreceptors and nerve endings and, therefore, reduced sensation below the electrodes enabling the user to focus on the referred sensation.

C. Effect of Electrode positions on IFS

Figures 1 (D) (i) and (E) (i) show the change in the maximum field intensity at the nerves with different ratios of $I_a : I_b$ while keeping the sum constant ($= 5$mA). The difference in the results obtained provides an insight into the sensitivity of IFS to the chosen electrode location. Despite

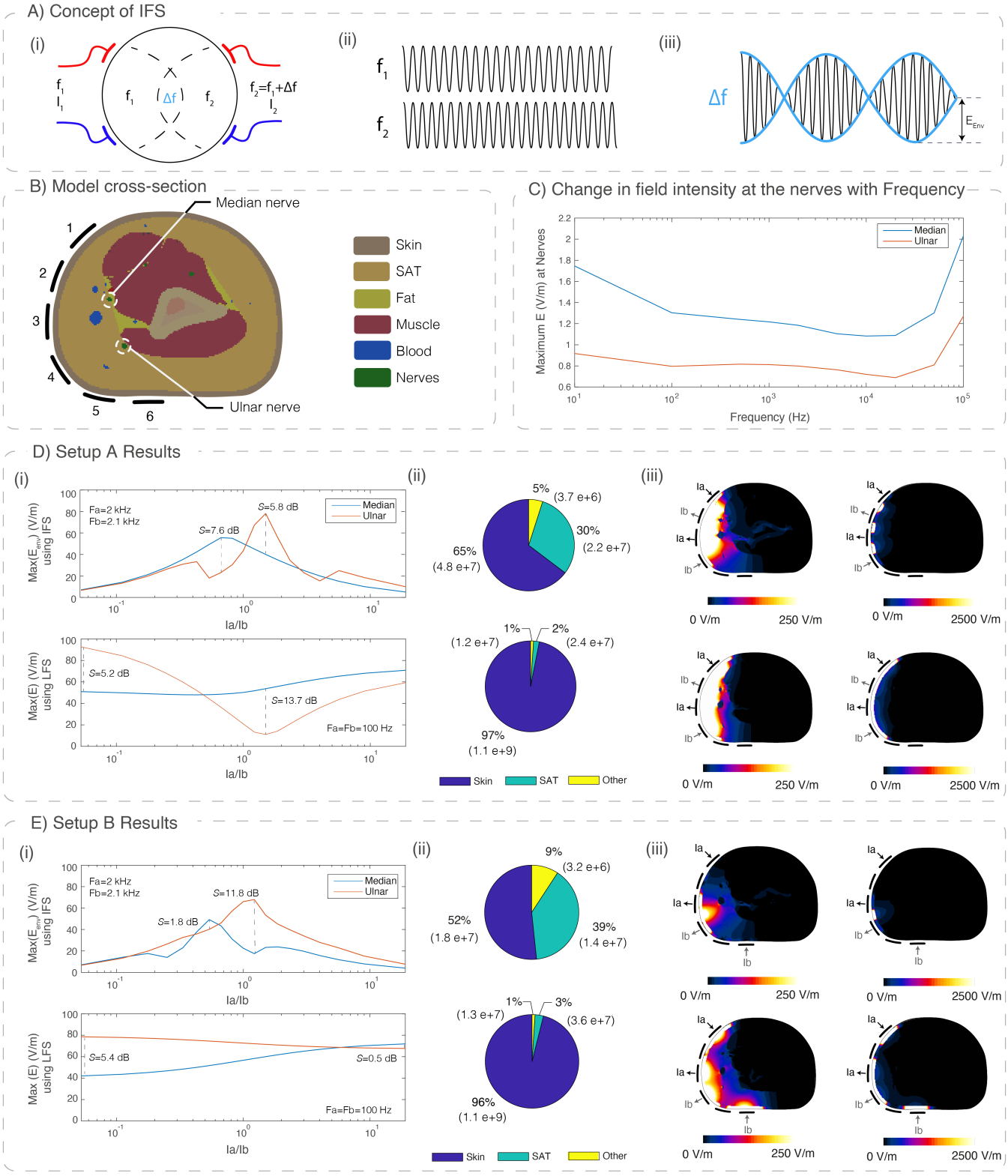

Fig. 1. A) (i) Simple IFS setup with two isolated circuits supplying electrical stimulation with frequencies f_1 and f_2 and stimulation currents I1 and I2. The region of interference follows the beat frequency, $f_2 - f_1$. (ii,iii) an illustration of the low frequency envelope produced by the two high frequency waveforms B)A cross section of the model voxels showing the different tissue and location of the Median and Ulnar nerves. C) The change in measured electric field intensity at the nerves with the applied frequency. D,E) The results obtained with setup A and B, respectively. (i) shows the change in maximum $\vec{E}$ as the ratio of I_a : I_b is changed (steps of 0.25mA) while keeping the total current constant. The values of the frequencies used are highlighted on the plots as well as the maximum sensitivity value for each nerve (ii) shows how the electric field is distributed between different tissues, highlighting the skin and SAT. The values between brackets are the sum of the magnitudes of the fields at each of the grid points. (iii,iv) slices of the simulation results showing the electric field intensity plotted on two different scales to isolate the field under the electrode from that within the arm. The electrodes used for each current (I_a and I_b) are shown using arrows.

the ability to 'steer' the target location, evident in the two peaks in the Ulnar and Median nerve plots, the selectivity and maximum field intensity achievable at each nerve is dependent on the chosen electrode location. For example, setup B resulted in higher selectivity using HFS than LFS. Setup A, on the other hand, showed opposite results in terms of selectivity of the Median nerve. Interestingly, the highest selectivity with LFS did not occur at the highest $I_a : I_b$ ratio as expected, showing that the ratio of currents between two pairs of electrodes could be used for LFS as well. The reason behind the increased selectivity with setup B can be visualised in the plots(iii). Increased separation between the electrodes in setup B enables the IFS field to be more focused than in setup A.

The disadvantage of increasing the separation between the fields is the need for higher currents. Comparing the maximum $\vec{E}$ obtained across the different current ratios for each stimulation method shows that the values obtained with LFS stimulation are generally higher, especially in setup B. This suggests that IFS may require higher currents than LFS. The increase in the required current can, however, be minimised by optimising the setup, as shown in setup A where the field intensity at the Median nerve was equal to 77.7V/m using IFS compared to 84.3V/m using LFS. The use of an array of electrodes can enable different pairs of electrodes to be used to stimulate the Median, Ulnar, or both nerves.

IV. Discussion and Conclusions

The results obtained show that using IFS for sensory feedback has the potential of enabling referred sensation to be elicited with reduced sensation below the electrodes as compared to LFS. Using IFS might require higher currents to be used; however, this is not necessarily a limitation as the reported currents used for electrotactile sensory feedback tend to be limited by pain thresholds, rather than safety limits which are higher. The reduced activation of mechanoreceptors could enable higher currents to be used without causing discomfort.

This preliminary study includes some limitations that will be addressed in future work. To start with, a larger number of setups has to be compared for a better assessment of the sensitivity of IFS to electrode locations. Selecting suitable locations to result in referred sensation using LFS is a time-consuming process. The steerability of IFS could enable faster setup, but this is reliant on its sensitivity to electrode position and the allowable current limtis. Moreover, it is unclear how anatomical variations between subjects could influence the chosen setup. This can be addressed by repeating the simulation using different computational models or using 3D scans from participants. Another area of improvement is using the F descriptor proposed by Li et al. as a more accurate representation of the sensation eliciting field than equation (1) [10]. Another improvement to the model would include a more realistic electrode-skin interface and, consequently, an adaptive grid. Finally, verification tests on physical phantoms and participants are required.

In conclusion, the paper has shown, through realistic a computational phantom model, that using IFS is a potential solution to reduce the local sensation felt below the electrodes when using electrotactile stimulation to elicit referred sensation.

Appendix: Current Calculation

The current was calculated using $I = P/V$ where V is the set voltage and P is the power loss at the peak current. Sim4life generates the average power loss in a sinusoidal field using equation (3) (where L is the total power loss within volume R, σ is the electric conductivity and E is the electric field phasor).

$$L(R) = \frac{1}{2}\int_R \sigma E \cdot E^* \, dv \tag{3}$$

The reason behind dividing the integral by two is that $E_{RMS} = E/\sqrt{2}$ is required to obtain the average power loss. Therefore, multiplying the generated power by two results in the power loss at the peak current. The peak current is then calculated using $I = 2L(R)/V$.

References

[1] J. W. Sensinger and S. Dosen, "A Review of Sensory Feedback in Upper-Limb Prostheses From the Perspective of Human Motor Control," 6 2020.

[2] H. Shin, H. Huang, Z. Watkins, Y. Zhu, and X. Hu, "Evoked haptic sensations in the hand via non-invasive proximal nerve stimulation," *Journal of Neural Engineering*, vol. 15, 5 2018.

[3] E. D'Anna, F. M. Petrini, F. Artoni, I. Popovic, I. Simanić, S. Raspopovic, and S. Micera, "A somatotopic bidirectional hand prosthesis with transcutaneous electrical nerve stimulation based sensory feedback," *Scientific Reports*, vol. 7, no. 1, pp. 1–15, 2017.

[4] E. Mirzakhalili, B. Barra, M. Capogrosso, and S. F. Lempka, "Biophysics of Temporal Interference Stimulation," *Cell Systems*, pp. 1–16, 2020.

[5] Y. Huang and L. C. Parra, "Can transcranial electric stimulation with multiple electrodes reach deep targets?," *Brain stimulation*, vol. 12, no. 1, pp. 30–40, 2019.

[6] L. E. Medina, "Quantitative Analysis of Kilohertz-Frequency Neurostimulation," 2016.

[7] M. Yoshida and Y. Sasaki, "Sensory feedback system for prosthetic hand by using interferential current," *Annual International Conference of the IEEE Engineering in Medicine and Biology-Proceedings*, vol. 2, pp. 1431–1432, 2001.

[8] K. Nomura, K. Yada, M. Saihara, and M. Yoshida, "Interferential current stimulation for sensory communication between prosthetic hand and man," *Annual International Conference of the IEEE Engineering in Medicine and Biology - Proceedings*, vol. 7 VOLS, pp. 6923–6926, 2005.

[9] N. Grossman, D. Bono, N. Dedic, S. B. Kodandaramaiah, A. Rudenko, H. J. Suk, A. M. Cassara, E. Neufeld, N. Kuster, L. H. Tsai, A. Pascual-Leone, and E. S. Boyden, "Noninvasive Deep Brain Stimulation via Temporally Interfering Electric Fields," *Cell*, vol. 169, no. 6, pp. 1029–1041, 2017.

[10] J. Li, K.-M. Lee, and K. Bai, "Analytical and Experimental Investigation of Temporal Interference for Selective Neuromuscular Activation," *IEEE Transactions on Neural Systems and Rehabilitation Engineering*, vol. 4320, no. c, pp. 1–1, 2020.

[11] M. C. Gosselin, E. Neufeld, H. Moser, E. Huber, S. Farcito, L. Gerber, M. Jedensjo, I. Hilber, F. D. Gennaro, B. Lloyd, E. Cherubini, D. Szczerba, W. Kainz, and N. Kuster, "Development of a new generation of high-resolution anatomical models for medical device evaluation: The Virtual Population 3.0," *Physics in Medicine and Biology*, vol. 59, pp. 5287–5303, 9 2014.

[12] P. Hasgall, F. Di Gennaro, C. Baumgartner, E. Neufeld, M. Gosselin, D. Payne, A. Klingenbock, and N. Kuster, "IT'IS Database for thermal and electromagnetic parameters of biological tissues," 2015.